Biosensors and Bioelectronics 141 (2019) 111411

Contents lists available at ScienceDirect

Biosensors and Bioelectronics

journal homepage: www.elsevier.com/locate/bios

Scanning electrochemical microscopy in the development of enzymatic sensors and immunosensors

Inga Morkvenaite-Vilkonciene[a,b], Almira Ramanaviciene[a,*], Aura Kisieliute[a,c], Vytautas Bucinskas[b], Arunas Ramanavicius[a,c]

[a] NanoTechnas – Center of Nanotechnology and Materials Science, Faculty of Chemistry and Geosciences, Vilnius University, Naugarduko 24, LT-03225, Vilnius, Lithuania
[b] Department of Mechatronics and Robotics, Vilnius Gediminas Technical University, J. Basanavičiaus 28, 03224, Vilnius, Lithuania
[c] Department of Physical Chemistry, Faculty of Chemistry and Geosciences, Vilnius University, Naugarduko 24, LT-03225, Vilnius, Lithuania

ARTICLE INFO

Keywords:
Scanning electrochemical microscopy
Enzymatic sensors
Immunosensors
Horseradish peroxidase
Alkaline phosphatase
Glucose oxidase

ABSTRACT

Scanning electrochemical microscopy (SECM) is very useful, non-invasive tool for the analysis of surfaces pre-modified with biomolecules or by whole cells. This review focuses on the application of SECM technique for the analysis of surfaces pre-modified with enzymes (horseradish peroxidase, alkaline phosphatase and glucose oxidase) or labelled with antibody-enzyme conjugates. The working principles and operating modes of SECM are outlined. The applicability of feedback, generation-collection and redox competition modes of SECM on surfaces modified by enzymes or labelled with antibody-enzyme conjugates is discussed. SECM is important in the development of miniaturized bioanalytical systems with enzymes, since it can provide information about the local enzyme activity. Technical challenges and advantages of SECM, experimental parameters, used enzymes and redox mediators, immunoassay formats and analytical parameters of enzymatic SECM sensors and immunosensors are reviewed.

1. Introduction

Scanning electrochemical microscopy (SECM) concept was introduced by A. J. Bard in 1989 (Bard et al., 1989) as a technique, which enables the visualization of local electrochemical activity of various surfaces. The SECM is based on electrochemical measurements performed by an ultramicroelectrode (UME), which can perform 3D scans of a space close to the surface of interest, which could contain catalytic, redox or other electrochemically active sites. In such experiments the UME is usually connected as a working electrode in an electrochemical setup, and the current, which is measured by the UME, depends on the local concentration of electroactive species and applied potential. The main advantage of SECM is that this technique can be applied for *in-situ* studies without any damage to the system of interest. It is very important in the development of enzymatic (Nogala et al., 2010) and affinity (Conzuelo et al., 2016; Ning et al., 2018) biosensors. In addition, the SECM can be used for high-resolution imaging of local chemical reactions (Wittstock et al., 2007; Teranishi, 2011; Huang et al., 2018) and topography of enzyme-based interfaces formed in immunoassays (Yasukawa et al., 2007), on the surface of biosensors or biochips (Zhao and Wittstock, 2005). SECM does not require the pre-treatment of biological sample, as it should be done if fluorescence or scanning electron microscopy are used for imaging (Roberts et al., 2007; Aranda et al., 2018; Lou et al., 2018). In addition, fluorescence technique creates artefacts from the background. SECM is a valuable technique because the mathematical models can be fitted to the results, obtained by the SECM and thus reaction kinetics can be evaluated (Sun et al., 2018; Ivanauskas et al., 2016). SECM can be used for: (i) the imaging of electrochemical processes at liquid/solid, liquid/gas and liquid/liquid interfaces (Lin et al., 2018; Kai et al., 2018; Barker et al., 1999), (ii) the characterisation and quantification of catalytic reactions and processes for enzymes immobilised on surfaces of different conductivity (Izquierdo et al., 2018; Morkvenaite-Vilkonciene et al., 2014), (iii) or for enzymes used as labels in the visualization of antigen and antibody interactions (Yang et al., 2018; Conzuelo et al., 2016). SECM was successfully applied as a complementary technique to others well known surface characterization techniques, such as atomic force microscopy (AFM), scanning tunnelling microscopy and surface plasmon resonance imaging. The bifunctional SECM–AFM probes were simultaneously used for the mapping of enzyme activity and imaging of immobilized enzyme spots with nanometric resolution (Kranz et al., 2004). Great improvement in lateral resolution can be achieved combining SECM with scanning tunnelling microscopy (Treutler and Wittstock, 2003). By combining SECM with surface plasmon resonance imaging it is possible

* Corresponding author.
E-mail address: almira.ramanaviciene@chf.vu.lt (A. Ramanaviciene).

https://doi.org/10.1016/j.bios.2019.111411
Received 26 March 2019; Received in revised form 24 May 2019; Accepted 3 June 2019
Available online 08 June 2019
0956-5663/

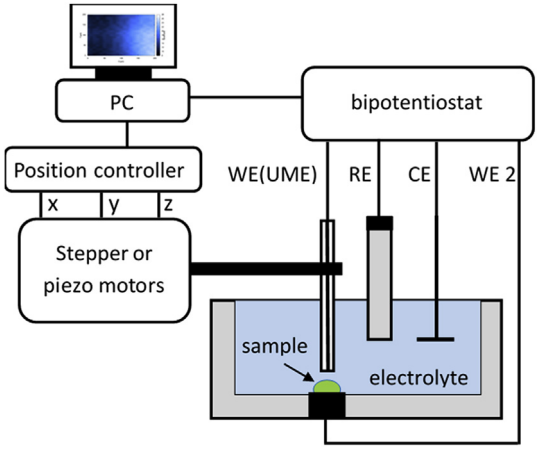

Fig. 1. Scheme of typical SECM experiments. WE (UME) – working ultramicroelectrode, RE – reference electrode, CE – counter electrode, WE 2 – substrate as a second working electrode. All electrodes are connected to the bipotentiostat.

to control surface patterning processes and get new information about the formation of micropatterns (Szunerits et al., 2004).

This review firstly focuses on the working principle and operating modes of SECM, secondly – on the application of SECM technique for the characterisation and quantification of local enzymatic activity of horseradish peroxidase (HRP), glucose oxidase (GOx) and alkaline phosphatase (ALP) immobilised on the surfaces and finally, on the enzymes used as labels during specific antigen and antibody interactions.

2. SECM working principle and operating modes

The main part of the SECM is the ultramicroelectrode (UME), with a diameter in the micrometer range, and it is usually used as a working electrode in an electrochemical cell. The UME can be moved in three directions and the current is registered as a function of the coordinates. The experimental SECM scheme is shown in Fig. 1. Here a four-electrode electrochemical cell is shown with the UME as a moving working electrode, reference and counter electrodes, and the substrate as a second working electrode. All electrodes are connected to the bi-potentiostat. The control and movement of the UME and also current registration at the same time are controlled and recorded by a specialized software. The steady-state diffusion-controlled current is related to the mediator's concentration (Bard and Mirkin, 2001):

$$i_{T,\infty} = 4nFDCa \quad (1)$$

where n is the number of electrons, which are involved in the reaction on the surface of the UME, F is the Faraday constant (9.65×104 C/mol), D is the diffusion coefficient, C is the concentration of the mediator, and a is the radius of the UME.

All SECM experiments can be carried out at constant height and at constant distance modes. In constant height mode the UME is moved only laterally in the x and y directions, while in constant distance mode the UME can be moved in x-y-z directions but remain at the same vertical distance from the sample. In this mode the UME current depends on the distance between the UME and the surface of interest and on the reactivity of the compounds immobilized on the surface. To determine the most suitable distance for the appropriate resolution of SECM in constant height mode measurement, the current *vs* distance dependence could be measured in feedback mode by approaching the UME to the surface of interest. The distance between the UME and the sample could be calculated from the SECM theory, where $i_T/i_{T,\infty}$ (ratio of UME current and steady-state current far from an electrochemically active surface) can be related to d/a (the ratio of distance between the sample and the UME radius). However, this approach is not accurate and can lead to the tip crashing or damaging the sample. These limitations can be resolved by using a shear-force based constant-distance control (Ludwig et al., 1995): the microelectrode vibrates at its resonance frequency with typical amplitudes of only a few nanometres with the use of a piezo-pusher (Hengstenberg et al., 2000). Simultaneously, a laser beam is focused onto the very end of the vibrating electrode and the resulting Fresnel diffraction pattern is projected onto a split photodiode. The amplitude and phase information about the vibrating tip is obtained by the amplification of the differences in signals from the split photodiode with respect to the agitation signal used by a lock-in amplifier. With the decreasing tip-to-sample distance, increasing the shear forces between the tip and the sample's surface leads to a damping of the vibration amplitude and to a phase shift, which can be used to continuously keep a predefined damping value related to a constant distance of about 50 ± 100 nm by means of a software-controlled feedback loop (Hengstenberg et al., 2000). Another method of the shear-force detection is accomplished by mechanically attaching a set of two piezoelectric plates to the scanning probe (Ballesteros Katemann et al., 2003). One of the plates is used to excite the SECM tip causing it to resonate, and the other acts as a piezoelectric detector of the amplitude of the tip oscillation. Increasing the shear forces in close proximity to the sample's surface lead to a damping of the vibration amplitude and a phase shift, effects that are registered by connecting the detecting piezoelectric plate to a dual-phase analogue lock-in amplifier (Ballesteros Katemann et al., 2003). Also, a shear force-based method is able to work at various tip-to-sample distances. It can hence detect complete diffusion profiles in the surroundings of sources or sinks of redox-active species (Nebel et al., 2010). In particular, coupling SECM with scanning probe techniques, such as atomic force microscopy (AFM) (Macpherson et al., 1996) and scanning ion conductance microscopy (SICM) (Comstock et al., 2010), shear force (Ballesteros Katemann et al., 2003; James et al., 1998; Ludwig et al., 1995) and impedance-based techniques (Alpuche-Aviles and Wipf, 2001), led to efficient strategies to control the tip-to-sample separation. In the combined technique of AFM-SECM, the AFM tip is used as a working electrode and as the force sensor at the same time (Eckhard et al., 2007; Shin et al., 2008). This technique allows to achieve the best resolution and to measure different properties of the surface.

2.1. Feedback modes

SECM feedback modes can be distinguished into two parts: negative feedback and positive feedback. Far from the surface, the current depends only on the concentration and diffusion of the redox species (Fig. 2). If the current decreases when the UME approaches the surface of interest, the resulting curve is of negative feedback behaviour (Fig. 2A). It happens if a surface is an insulator. If the current increases when the UME approaches the surface, the resulting curve is of a positive feedback behaviour (Fig. 2B) and can be achieved approaching a conducting surface. When the UME approaches biological objects, negative feedback can only be achieved if no redox reaction occurs. Then the current depends only on the distance from the surface.

In positive FB-SECM mode the current increases when the UME approaches a conducting surface of interest. Moreover, the registered current at positive FB mode could increase even when the conducting surface, which is evaluated by SECM, is not connected to the potentiostat (Bard et al., 1992). In this case the redox compounds, which are generated on the UME participate in an opposite oxidation-reduction reaction on the conducting surface, creating a regenerative “positive” feedback loop (Bard et al., 1992). Due to this reaction, the concentration of compounds, which are utilized by the UME, increases close to the conducting surface. However, such reversible redox process can be observed only when the UME is close (at the distance equal to 1–2 radii of the UME) to the conducting surface.

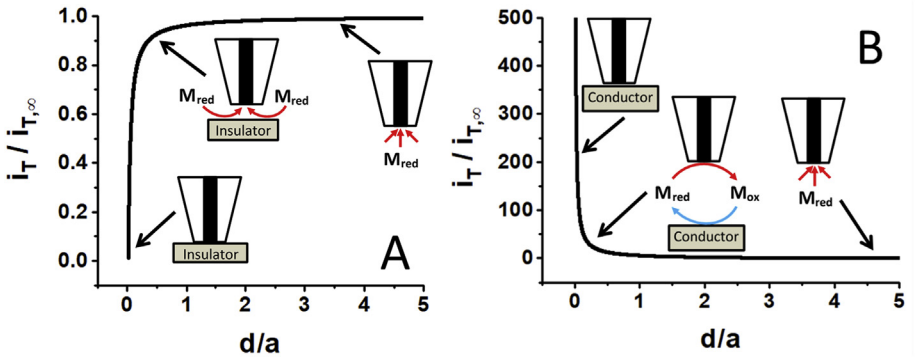

Fig. 2. A – Negative feedback (hindered diffusion) mode when the UME is approaching the insulating surface; **B** – Positive feedback mode when the UME is approaching a conducting surface. Negative feedback curve was calculated by Cornut and Lefrou equation (Cornut and Lefrou, 2007) using RG = 10; positive feedback curve was calculated by Cornut and Lefrou equation (Cornut and Lefrou, 2008) using RG = 10 and Λ = 1.

2.2. Generation-collection modes

The GC-SECM mode is characterized by a relatively high sensitivity compared to other modes of the SECM. Therefore, GC-SECM mode is suitable for the detection of small quantities of electro-active species, which are diffusing out from immobilized biological objects. In addition, the UME at GC-SECM mode is used as a passive sensor, which has minimal distortions to the surface of investigation. In GC-SECM mode, the UME is only registering currents, which are caused by the reaction products (Gyurcsányi et al., 2004; Shiku et al., 2001; Wittstock, 2001). Usually the UME passively detects the redox compounds, which are generated at the surface of interest. The problem is that the reaction in the sample occurs continuously, independently of the presence/absence of the UME. There are two SECM generation-collection modes: Substrate generation/Tip collection (SG/TC) (Fig. 3A) and Tip generation/Substrate collection (TG/SC) (Fig. 3B).

In the SG/TC mode, the solution initially contains redox species, which are not yet detectable. If these redox species were oxidized/reduced by the sample, then the oxidized/reduced forms would be detected by the UME. In the TG/SC mode, the UME is generating electroactive species, which could be detected on a conducting surface of interest, which in such investigation should be switched as one of the electrodes of a particular electrochemical circuit. If the redox species are detected on the UME, and at the same time consumed in the reaction near the surface of interest, such type of mode is called 'Redox competition' mode (RC-SECM) (Fig. 3C).

2.3. Redox competition mode

The RC-SECM mode, which was developed by Schumann's group (Eckhard et al., 2006), could be used for evaluating the oxygen reduction reaction (Fig. 3 C). The advantage of this mode is that the enzymes can be investigated in solution without redox mediators, since only oxygen reduction current is registered. The monitoring of catabolism by measuring oxygen consumption is a commonly used technique, and the redox competition mode of SECM can be applied for this purpose (Nebel et al. 2013a, 2013b). These experiments were performed in bipotentiostatic mode, when the surface of interest was connected to the potentiostat and particular potential was applied. For the evaluation of conducting surfaces modified by enzymes, the oxygen consumption rate can be registered. In this case, the dissolved oxygen is consumed in two competing reactions: one is occurring on the UME and another one – on the surface modified by an enzyme (e.g. GOx), which is utilizing O_2 as an electron acceptor (Morkvenaite-Vilkonciene et al., 2014). In RC-SECM mode the consumption rate on the UME is much slower than that on the surface of interest. Therefore, in this mode the 'competition' is doubtful, and in most cases using this mode it is possible to measure the rate of consumption of redox active species on the surface. The advantage of this mode is that the redox mediator can be not even present in the solution, for example, to measure oxygen consumption by enzymes, which utilize oxygen. The approach curves in this mode will be characterized by a 'negative feedback' behaviour, therefore, the comparison of the results with the approach curve, observed measuring insulating surface is needed. To determine kinetics of the enzyme from RC-SECM mode measurements, a good way is to plot current *vs* substrate concentration dependencies at different distances and then apply Michaelis-Menten kinetics (Morkvenaite-Vilkonciene et al. 2017b). Apparent Michaelis constant of superposition of redox and diffusion processes can be calculated and it depends on the distance between the UME and the surface of interest (Morkvenaite-Vilkonciene et al., 2014). However, the 'real' Michaelis constant value can be determined only at distances, where hindered diffusion does not occur. The mathematical models can be applied in order to calculate oxygen consumption rate and diffusion coefficients from experimental results

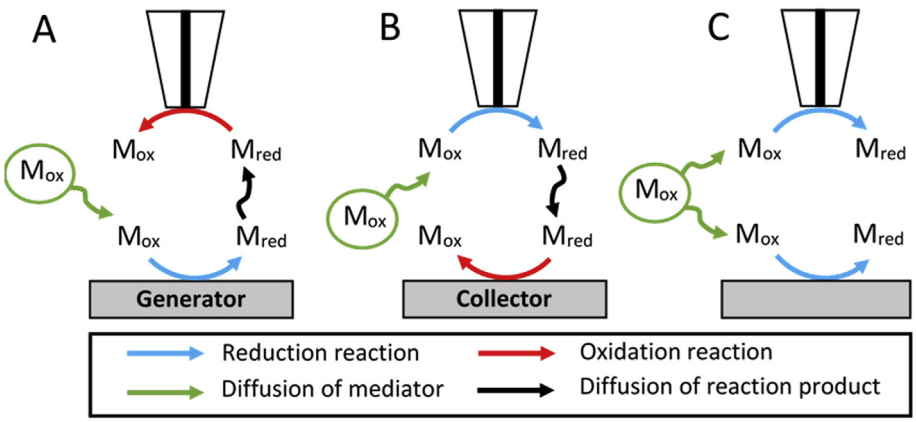

Fig. 3. Generation-collection mode of SECM: **A** – species, generated by the substrate electrode, are collected by the UME; **B** – UME generated species are collected by the substrate electrode. Redox competition mode of SECM: **C** – species are detected on the UME, and at the same time are consumed on the substrate electrode.

obtained using RC-SECM mode (Ivanauskas et al., 2016). Additionally, mathematical models can be used for the evaluation of UME geometry influence on registered signal (Astrauskas et al., 2019).

The selection of the best SECM mode depends on the object of interest, the properties, which will be investigated, and on the measuring conditions, which are necessary to achieve the goal.

3. Application of SECM in enzymatic sensors and immunosensors

3.1. Enzymes

Many articles have been published about the research of enzyme-modified surfaces using SECM-based techniques. The most popular and widely used enzymes in biosensor related field of research are oxidoreductases (Wittstock, 2001). For the detection of these enzymes GC-SECM mode is commonly used. GC-SECM mode is more favourable than FB-SECM mode due to higher registered current and possibility to investigate at higher distances from the surface. Measurements can be done at distances higher than 10 UME radii without the risk to damage the immobilized enzyme or to break the electrode. Although in GC-SECM mode the reaction on the surface of interest becomes steady-state only after a certain period of time after the addition of the substrate into an electrolyte. It should be noted that in order to get more reliable measurement results it is necessary to wait until the current stabilizes before each SECM measurement.

In order to determine the enzymatic kinetics in GC-SECM mode, the only way is to increase the concentration of the substrate and to measure the current. Further calculations from the registered current dependences on the substrate concentration are performed. The easiest way to determine enzymatic kinetics is by vertical approaching to the immobilized enzyme using FB-SECM or RC-SECM modes, e.g. to measure current *vs* distance dependencies and apply mathematical models for kinetic calculations (Burchardt et al., 2009; Cornut et al., 2009; Ivanauskas et al., 2016). Mathematical models have been created for SECM-based evaluation of enzymatic redox reactions in the presence of redox mediators. The selection of appropriate mediator is one of the most important issues in enzymatic, antigen-antibody interactions and other studies using the SECM. Therefore, in this review the imaging and the evaluation of enzymatic reactions kinetics at optimal experimental conditions are discussed separately for HRP, ALP and GOx enzymes.

The immobilization of enzymes is a very important issue in the development of biosensors. Proper immobilization of enzyme molecules can retain and sometimes even enhance the activity of enzymes and improve operational stability (Mohamad et al., 2015). Usually for the research by SECM enzymes are immobilized on the surface in small spots with a diameter of about 100–200 μm. To form such small spots different techniques can be exploited. The protein's amino acids can be involved in the binding of the enzyme to the support through various types of interactions, for example, hydrogen bonds, ionic binding, hydrophobic interactions, van der Waals forces, affinity binding or the formation of covalent bonds (Brena et al., 2013). Covalent linkage *via* cross-linking with polymers ensures strong binding of the enzyme to the electrode's surface, but the denaturation of the enzyme might occur if excess of cross-linking agent is used (Khan and Wernet, 1997). Immobilisation of enzymes through weak, non-specific forces and interactions is a simple method, however these enzymes can still detach from the surface even under gentle conditions (Zhou et al., 2002). SECM is able to detect changes in the electrochemical reaction kinetics (Zhou et al., 2002) and, at the same time, changes in the enzyme's activity, depending on the used immobilization method. To ensure that the changes in the electrical current are caused by the reaction catalysed by the enzyme (but not by the reaction between the substrate and the redox mediator), cyclic voltammograms have to be registered with the redox mediator in presence and absence of the substrate and in the absence of the enzyme (Zhou et al., 2002). The obtained results should be similar independent of the presence or absence of the substrate in the solution. It means that the reaction of the substrate and the mediator is very slow and the changes in the registered current close to the enzyme's surface will be detected due to the enzyme-catalysed reaction.

3.1.1. Horseradish peroxidase

The first attempt to investigate the HRP applicability in SECM investigations was made in 1993 (Horrocks et al., 1993). The UME modified by HRP and a redox polymer was used for the determination of hydrogen peroxide concentration, which was formed during GOx catalysed enzymatic oxidation of glucose. Amperometric registration of HRP activity can be carried out by using a variety of different redox mediators, such as ferrocene and its derivatives, quinone and redox dyes (Laschi et al., 2009; Li et al., 2008; Loaiza et al., 2008). The HRP catalysed enzymatic reaction at −0.2 V *vs* Ag/AgCl in the presence of 1 mM H_2O_2 in the solution was investigated by a carbon macroelectrode using three different redox mediators: 1.0 mM ferrocene methanol (FcMeOH), 1.0 mM ferrocene carboxylic acid (FeCOOH), and 1.0 mM hydroquinone (H_2Q) (Laschi et al., 2009). About a 3 times higher current was registered using 1.0 mM H_2Q in comparison to the other two (FcMeOH and FeCOOH) redox mediators. Therefore, this redox mediator is a promising candidate in the SECM research. Different redox mediator forms can be used depending on the selected SECM mode (Fig. 4). The reactions on the UME and HRP stay the same in both previously mentioned modes (Eq. (2) and (3)), but in GC-SECM mode the H_2Q is added to the solution, while in FB-SECM mode the BQ is added to the solution. In the GC-SECM mode after introducing H_2Q, the molecule is oxidized to BQ on the enzyme-modified surface in the presence of H_2O_2, thus, BQ is generated on the enzyme modified surface during measurements (Fig. 4A). The UME is sensitive towards different concentrations of produced BQ at the potential −400 mV *vs* Ag/$AgCl/_{3\,M\ KCl}$ (Conzuelo et al., 2014). In FB-SECM mode the BQ is added in the electrolyte and H_2Q is produced after the reduction of BQ on the UME at −400 mV vs $Ag/AgCl/_{3\,M\ KCl}$ (Fig. 4B). The reversible reaction (oxidation of H_2Q to BQ) will take place on the enzyme modified surface in the presence of H_2O_2 (Zhou et al., 2002). In this case, the background current generated by the presence of BQ in the solution has increased at close distance to the surface. By comparing these two SECM modes, it is evident that in GC-SECM mode the enzyme-catalysed reaction in the presence of H_2O_2 occurs all the time, while in FB-SECM mode this reaction starts only when the UME is close to the enzyme's surface and after H_2Q is produced. Therefore, the imaging in FB-SECM mode should be performed at a distance, which is several times closer to the enzyme modified surface, rather than in GC-SECM mode. For example, the distance for HRP imaging by FB-SECM was performed at 5 μm distance, while in GC-SECM mode this distance could be 15 μm

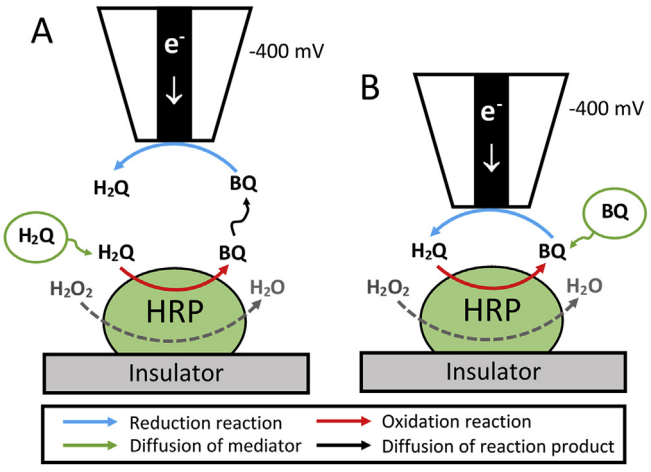

Fig. 4. Schematic representation of HRP detection using H_2Q/BQ as redox mediators using GC-SECM mode (A) or FB-SECM mode (B).

Table 1
Scanning electrochemical microscopy in the development of enzymatic sensors using different enzymes.

Sample	Concentration of substrate (H_2O_2)	Concentration of redox mediators	SECM mode/ probe/ diameter	Potential of UME probe *vs* Ag/AgCl	Scanning parameters	Ref.
			Horseradish peroxidase			
HRP/hydrogel on glass slide Polycarbonate filter membrane pores (14 μm) filled with the HRP/hydrogel Biotin-labelled HRP bound to avidin immobilised on glass slide	1 mM	1 mM BQ	FB-SECM carbon fibre 7μm	F02D0.4 V	Approach curves Imaging at 5 μm distance	(Zhou et al. 2002)
Streptavidin–HRP captured by double-stranded DNA modified gold *via* biotin–streptavidin interaction	1 mM	1 mM H_2Q	GC-SECM Pt 10 μm	F02D0.3 V	Imaging at 15 μm distance	(Zhang et al. 2010)
Streptavidin–HRP-labelled SiO_2 nanoparticles linked to the "sandwich" structure of DNA on the gold through streptavidin–biotin interaction	1 mM	1 mM H_2Q	GC-SECM Pt 10 μm	F02D0.4 V	Approach curves Imaging at 15 μm distance	(Fan et al. 2013)
HRP immobilised on amino-modified glass slide using glutaraldehyde crosslinking	1, 0.6, 0.4 or 0.2 mM	1mM H_2Q	GC-SECM Pt –	F02D0.4 V	Approach curves Imaging at 50 μm distance	(Roberts et al. 2011)
Avidin-HRP bound to polymer formed on gold and modified with biotin or poly (propylene glycol)	1 mM	2 mM FcMeOH	GC-SECM Pt 9 μm	F02D0.05V	Imaging at 10 μm distance	(Glidle et al. 2003)
HRP bound to amino functionalised gold surface	0.5 mM	2 mM FcMeOH	GC-SECM Pt 25μm	0 V	Imaging at 10 μm distance	(Wilhelm and Wittstock 2003)
			Alkaline phosphatase			
Sample	Concentration of substrate (4-aminophenyl phosphate)	Concentration of redox mediators	SECM mode/ probe/ diameter	Potential of UME probe *vs* Ag/AgCl	Scanning parameters	Ref.
ALP in the mouse embryonic stem cells	4.7 mM PAPP	–	GC-SECM Pt 10 μm	+0.30 V	Imaging at 20 μm distance	(Arai et al. 2013)
ALP in the human breast cancer cells	5 mM PAPP	–	GC-SECM Pt 10 μm	+0.30 V	Imaging at 30 μm distance	(Torisawa et al. 2006)
			Glucose oxidase			
Sample	Concentration of substrate (glucose)	Concentration of redox mediators	SECM mode/ probe/ diameter	Potential of UME probe *vs* Ag/AgCl	Scanning parameters	Ref.
1. GOx covalently bounded to Nylon; 2. GOx in hydrogel membranes; 3. GOx immobilized in Langmuir-Blodgett (LB) films	50 mM	0.05- 2 mM FcCOOH 0.05- 2 mM $K_4[Fe(CN)_6]$ 0.02- 2 mM H_2Q	FB-SECM carbon 8 μm	F02D F02D F02D	Approach curves	(Pierce et al. 1992)
Streptavidin-coated magnetic beads modified by biotinylated GOx	50 mM	1 mM dimethylaminomethyl ferrocene	FB-SECM Pt 10 μm	+0.4V	Imaging at 25 μm distance	(Wijayawardhana et al. 2000b)
GOx immobilised on amino-functionalised gold surface	50 mM	–	GC-SECM Pt 50μm	+0.4V*	–	(Wittstock and Schuhmann 1997)
GOx immobilised on amino-functionalised glass slide using glutaraldehyde crosslinking	50 μM – 1 mM	–	GC-SECM carbon 20 μm	+0.8V	Imaging at 30 μm distance	(Kasai et al. 2002)
GOx solution immobilised with Cellophane membrane or GOx entrapped in poly-acrylamide gel membrane	0.2–4 mM	–	GC-SECM Pt 25μm RC-SECM Pt 25μm	+0.6 V −0.6 V	Approach curves Approach curves	(Csoka et al. 2003)
SATA-GOx conjugate on gold	50 mM	–	GC-SECM Pt 25μm	+0.75 V	Imaging at 40 μm distance	(Wilhelm and Wittstock 2003)
Biotin-GOx/avidin/biotin-polypyrrole on platinum substrate	9.9 mM	–	GC-SECM Pt 25μm	+0.6 V	Imaging at 10 μm distance	(Evans et al. 2005)

(*continued on next page*)

Table 1 (*continued*)

Sample	Concentration of substrate (H_2O_2)	Concentration of redox mediators	SECM mode/ probe/ diameter	Potential of UME probe *vs* Ag/AgCl	Scanning parameters	Ref.
Multilayer films of GOx and poly(dimethyl diallyl ammonium chloride)	10–100 mM	0.045-0.9 mM FcMeOH	FB-SECM Pt 25μm	+0.3 V	Approach curves	(Burchardt and Wittstock 2008)
GOx spotted on the polyethylene substrate and cross-linked with glutaraldehyde	25 mM	–	GC-SECM Pt 10 μm	+0.05 V	Imaging at 20 μm distance	(Li and Yu 2008)
GOx grafted in covalently attached and cross-linked hydrogel deposited on premodified glassy carbon electrode	30 mM	1 mM FcMeOH	FB-SECM Au 9 μm	+0.5 V	Approach curves	(Pellissier et al. 2008)
GOx in a polymer hydrogel matrix on the top of PB-modified glassy carbon electrode**	100 mM	–	RC-SECM Pt 25 μm	−0.6 V ***	Imaging at 10–18 μm distance	(Guadagnini et al. 2009)
A droplet of GOx-polymer solution on premodified hydrophobic glass slide	100 mM	–	GC-SECM Pt 250 μm	+0.65 V	Imaging at 50 μm distance	(Lei et al. 2009)
GOx immobilised on amino-functionalized glass slide	506 U/mL MUT and, 100 mM sucrose****	0.2 mM FcMeOH	– Pt-INV 25 μm	+0.05 V	Approach curves	(Gdor et al. 2013)
GOx entrapped within the polymer spot on glass slide	33 mM 100 mM	–	GC-SECM Pt 10μm 25μm	+0.65 V +0.7 V	Imaging at 10 μm distance	(Schafer et al. 2013)
GOx immobilised on poly(methyl methacrylate) surface using glutaraldehyde	0-30 mM 10 mM	–	RC-SECM GC-SECM	−0.6 V +0.6 V	Approach curves Imaging at 40 μm distance	(Morkvenaite-Vilkonciene et al. 2014)
	100 mM	–	Localized EIS Pt 10μm	0 V	Approach curves	(Morkvenaite-Vilkonciene et al. 2015)
	0-82.6 mM	–	RC-SECM Pt 200 μm	−0.75 V	Approach curves	(Morkvenaite-Vilkonciene et al. 2017b)

PAPP - p-aminophenylphosphate monosodium salt; FcCOOH - ferrocenecarboxylic acid; FcMeOH – ferrocenemethanol; * *vs*. calomel reference electrode (SCE); SATA – S-acetylthioglycolic acid N-hydroxy succinimidyl ester; ** Prussian Blue modified UME; *** four-electrode electrochemical cell with a Pt microelectrode (diameter 25 μm) and the modified GC plate as the working electrodes (probe and substrate, respectively); **** sucrose is cleaved to glucose and fructose by enzyme invertase (INV) and enzyme mutarotase (MUT) present in the solution transform α- to β-glucose; Pt–INV–Pt microelectrode modified by enzyme invertase.

(Zhang et al., 2010) or more.

3.2. Hydroquinone/benzoquinone redox mediators' system

Reaction on the UME:

$$BQ + 2H^+ + 2\bar{e} \rightarrow H_2Q \quad (2)$$

Reaction, catalyzed by HRP

$$H_2O_2 + H_2Q \xrightarrow{HRP} 2H_2O + BQ \quad (3)$$

3.2.1. Alkaline phosphatase

Alkaline phosphatase is an enzyme, which is expressed in many living organisms including humans. ALP detection by SECM was performed in GC-SECM mode using substrate 4-aminophenyl phosphate monosodium salt (PAPP) (Table 1). ALP is a biomarker of bone formation (Kuo and Chen, 2017), alveolar type II cell differentiation (Edelson et al., 1988), and orthodontic tooth movement using self-ligating brackets systems (Abdul Wahab et al., 2014). This enzyme has been used as a label in different immunoassays and for the development of electrochemical biosensors and immunosensors. ALP catalyses hydrolysis of the redox-inactive PAPP to the redox-active 4-aminophenol (PAP), which shows good electrochemical properties: such as i) low oxidation potential (+300 mV vs. Ag/AgCl), ii) negligible electrode fouling, and iii) reversible electrochemical behaviour (Tang et al., 1988). Reaction, catalyzed by ALP:

$$PAPP \xrightarrow{ALP} PAP$$

Reaction on the UME:

$$PAP \xrightarrow{+0.3\ V} QI + 2H^+ + 2\bar{e}$$

where QI is quinone imine.

Only the GC-SECM mode has been used for the imaging of ALP because PAP, a redox-active product of enzymatic reaction, is registered and the reversible reaction of PAP to PAPP does not occur on the UME, which is the necessary condition for FB-SECM mode (Wittstock et al., 1995). Application of this mode leads to low lateral resolution of obtained image, but the sensitivity is much higher than that in FB-SECM mode. Another advantage is that imaging using the GC-SECM mode is performed at relatively high distances from the surface compared with the FB-SECM, hence it is possible to reduce the probability to crash the UME tip or to damage the sample.

3.3. Glucose oxidase

Glucose oxidase is the enzyme, which is mostly used in enzymatic biosensors. The first application of SECM in order to determine the electrochemical activity of GOx was performed in 1992 (Pierce et al., 1992). In this research authors used three redox mediators: FcCOOH, potassium ferrocyanide ($K_4[Fe(CN)_6]$), and H_2Q at low concentrations (0.02–2.0 mM) and performed vertical approaching of the UME towards the surface of interest, which was modified by the immobilized enzyme at concentrations from 0 to 50 % wt.

Later, SECM was used to make microscopic enzymatically active GOx spots on self-assembled monolayer (SAM) of alkanethiolates formed on gold. GOx was imaged without redox mediators in GC-SECM mode. The electrochemical enzymatic glucose sensor, designed using GOx as a recognition element, had the ability to detect low glucose

Table 2
Scanning electrochemical microscopy in the development of immunosensors.

Capture antibody support/ immobilisation method	Immunoassay format/ labelled antibody or antigen	Redox mediator or substrate of enzyme/ potential	SECM mode/tip/ diameter	Tip-substrate distance/ scan rate	Limit of detection/ limit of quantification/ linear range	Ref.
Monoclonal goat anti-digoxin antibody covalently immobilised on glass substrate	Direct detection bound digoxin-ALP	4 mM PAPP +0.28 V *vs* Ag/AgCl/3M KCl	GC-SECM/ Pt 30 μm	10-20 F06Dm 7.9 F06Dm/s	– – –	(Wittstock et al. 1995)
Anti-CEA antibody adsorbed on silanised glass substrate	Direct sandwich anti-CEA-HRP antibody	1.0 mM $FcMeOH^+$ or 1.0 mM FcMeOH +0.05 V *vs* Ag/AgCl	FB-SECM or GC-SECM Pt 15 μm	– 9.8 F06Dm/s	F07E10[4] CEA molecules in a single 20 F06Dm radius spot – –	(Shiku et al. 1996)
Anti-HCG and anti-HPL antibodies adsorbed on the microfabricated silanised glass substrate	Direct sandwich/ anti-HCG-HRP and anti-HPL-HRP antibodies	1.0 mM FcMeOH +0.4 V or +0.05 V *vs* Ag/AgCl/KCl_{sat}	GC-SECM Pt 15 μm	– 9.8 F06Dm/s	0.1 IU/mL of HCG 3 ng/mL of HPL – –	(Shiku et al. 1997)
Anti-leukocidin antibody immobilised *via* affinity interaction with protein A-coated on glass substrate (antibody chip)	Direct sandwich/ biotin labelled anti-leukocidin antibody/ avidin labelled HRP	1.0 mM FcMeOH +0.05 V *vs* Ag/AgCl	GC-SECM carbon 20 μm	10 or 50 F06Dm 48.8 F06Dm/s	sample volume 10 μL 5.25 pg/mL leucocidin – –	(Kasai et al. 2000)
Anti-AFP, anti-CEA, anti-NSE, anti-Cyfra21-1 antibodies immobilised on biochip	Direct sandwich/ anti-AFP-HRP, anti-CEA-HRP, anti-NSE-HRP, anti-Cyfra21-1-HRP antibodies	1.0 mM H_2Q −0.4 V *vs* Ag/AgCl/3M KCl	GC-SECM/ Pt 25 μm	10 F06Dm 5 F06Dm/s	0.40 ng/mL of AFP, 0.42 ng/mL of CEA, 0.67 ng/mL of Cyfra21-1, 0.69 ng/mL of NSE – 5 ng/mL – 1 μg/mL for target proteins	(Ning et al. 2018)
Biotinylated anti-mouse IgG antibody immobilised *via* affinity interaction on streptavidin coated magnetic beads	Direct sandwich/ anti-mouse IgG antibody-ALP	4 mM PAPP +0.29 V *vs* Ag/AgCl	GC-SECM/ Pt 10 μm	70 F06Dm 8 F06Dm/s	0.25 ng or 1.4 F0B4 10^{-15} M of mouse IgG 6.4F0B4 10^{-11} M of mouse IgG –	(Wijayawardhana et al. 2000a)
Anti-PG1 and anti-PG2 antibodies adsorbed on hydrophobic glass substrate	Direct sandwich/ anti-PG1-HRP and anti-PG2-HRP antibodies	1.0 mM FcMeOH +0.05 V *vs* Ag/AgCl/KCl_{sat}	GC-SECM/ carbon 10 μm	50 F06Dm 24.4 or 48.8 F06Dm/s	1.6 ng/mL PG1 and PG2 – 12.8-50.5 ng/mL for PG1 12.8-40.4 ng/mL for PG2	(Yasukawa et al. 2007)
Anti- sulfapyridine antibody immobilised *via* affinity interaction with protein G present on glassy carbon plate	Direct competitive sulfapyridine-HRP antigen	1.0 mM H_2Q −0.4 V *vs* Ag/AgCl/3M KCl	GC-SECM/ carbon fiber 5-8 μm	15 μm 20 F06Dm/s	0.13 ng/mL sulfapyridine in milk – 0.5-56 ng/mL	(Conzuelo et al. 2014)
	Direct competitive sulfapyridine-HRP antigen and *in situ* deposition of AgNPs	5 mM hexacyanoferrate(III) +0.6 V *vs* Ag/AgCl/3M KCl	GC-SECM/ carbon fiber 5-8 μm	100 μm 5 F06Dm/s	– – –	(Conzuelo et al. 2016)
Anti-CD10 antibody adsorbed on a gold electrode	Direct sandwich gold nanoparticles as carrier for the detecting anti-CD10 antibody and HRP	1 mM hexacyanoferrate(III) and hexacyanoferrate(II) –	GC-SECM Pt 10 μm	– –	4.38 F0B4 10^{-12} M of CD10 antigen – 1.0 F0B4 10^{-11} - 6.0 F0B4 10^{-11} M	(Song et al. 2012)
Anti-IL-1F062 antibody adsorbed on premodified hydrophobic glass slide	Direct sandwich anti-IL-1F062-HRP	1 mM FcMeOH +0.05 V vs Ag/AgCl	– Au 200 μm Pt 10 μm	– 50 μm – 10 μm 24.4 μm/s	– – quantitative evaluation of IL-1F062 at 10-350 pg/mL	(Kasai et al. 2006)
Microscopic agglomerates of paramagnetic beads modified with anti-mouse antibodies	Direct detection anti-mouse IgG-ALP	4 mM PPAP +0.29 V vs Ag/AgCl	GC-SECM Pt 10 μm	45 μm 8 F06Dm/s	– – –	(Wijayawardhana et al. 2000b)

PAPP – 4-aminophenyl phosphate; FcMeOH – ferrocenemethanol; H_2Q – hydroquinone; PEG1 - pepsinogen 1; PEG2 - pepsinogen 2; AFP – alpha-fetoprotein; CEA – carcinoembryonic antigen; NSE – neuron-soecific enolase; Cyfra21-1 – cytokeratin-19-fragment; IL – interleukin.

concentrations (from 50 μM to 1 mM) by measuring an H_2O_2 oxidation current by the UME (Kasai et al., 2002). SECM can also be used in biosensor-related researches when H_2O_2 is produced and/or O_2 is consumed during enzymatic reactions, both are determined by changing the potential applied to the UME (Csoka et al., 2003; Morkvenaite-Vilkonciene et al., 2014). SECM is also suitable for the investigation of multienzyme layers, which are based on GOx and HRP immobilized on the solid substrate surface (Wilhelm and Wittstock, 2003). It was demonstrated that SECM is suitable for fabrication, functionalization and characterization of biologically active microspots (Evans et al., 2005)

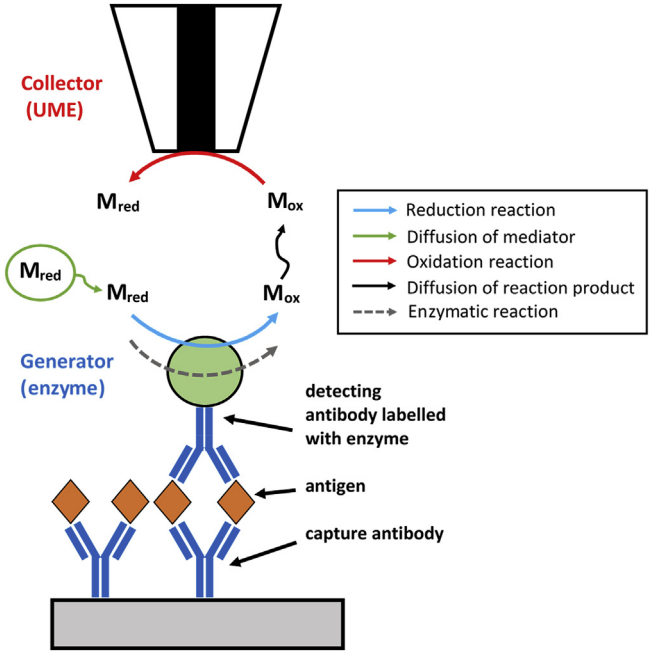

Fig. 5. Schematic representation of HRP-labelled antibody detection in GC-SECM mode.

and for reagentless determination of GOx (Li and Yu, 2008). This modification increases the sensitivity and spatial resolution when H_2O_2 is measured. SECM was combined with electrogenerated chemiluminescence (ECL) for advanced mapping of GOx. Hydrogen peroxide formed during the GOx-catalyzed reaction interacts with oxidized luminol that was simultaneously electrochemically generated at UME positioned in close proximity to GOx-modified surface (Lei et al., 2009). It was demonstrated that GOx also can be imaged in RC-SECM mode by measuring oxygen consumption during the enzyme-catalyzed reaction (Guadagnini et al., 2009; Morkvenaite-Vilkonciene et al. 2017b). In this case, the current is lower at the enzyme-modified surface area compared to the background current.

To evaluate enzymatic reaction kinetics, mathematical models, which were developed for approach curves measured by the FB-SECM mode are used (Burchardt and Wittstock, 2008; Gdor et al., 2013; Pellissier et al., 2008; Pierce et al., 1992). There is no possibility to create a mathematical model for enzymatic kinetics evaluation in GC-SECM mode, since the enzyme-catalyzed reaction starts immediately after glucose addition to the solution and the registered current changes in time. In FB-SECM mode the current is registered when the UME is at very close distance to the enzyme. In this case, the solution has to be deoxygenated. These mathematical models are suitable only in solutions with redox mediators, which have the ability to regenerate on the surface modified with the enzyme. The RC-SECM mode could be used for the determination of enzyme-catalysed reaction kinetics in solution without redox mediators (Ivanauskas et al., 2016). Here, the current registered using RC-SECM mode at a long distance from the enzyme modified surface changed with glucose concentration in the solution. Mathematical model shows that this phenomenon is observed when the diffusion coefficient of the oxygen becomes lower due to the high viscosity of the glucose solution so it becomes more difficult for the oxygen to reach the UME. Another research employed magnetic beads coated by streptavidin after reaction with biotinylated GOx for imaging with SECM by using FB-SECM mode (Wijayawardhana et al., 2000b). It was observed that the superior lateral resolution can be achieved, however, the sensitivity was limited due to high background current.

3.4. Antigen and antibody complexes

The possibilities and advantages of SECM in the imaging of enzyme-modified surfaces using electrochemical and enzymatic reactions can be successfully adapted for the detection of antigen and antibody interaction at localized surface areas. SECM is a better technique than spectroscopy and ellipsometry, which can be used for determination/evaluation of proteins on the surface but do not indicate or map their exact location (Wittstock et al., 1995). The common electrochemical methods applied for analyte determination using immunosensors have some disadvantages, since: i) the immobilization of biomolecules, specific interaction between the antigen and the antibody, washing steps and electrochemical detection occur on the same surface (electrode); ii) it is difficult to reuse electrochemical immunosensors due to the loss of activity of antigens or antibodies after the immobilization on a metal surface or due to partial regeneration of surface after electrochemical analyte determination, whereas for a single-use such a system is too expensive (Ramanaviciene et al., 2012); iii) the biomolecules on the electrode's surface slow down the diffusion of redox species and the charge transfer (the electrode might be 'blocked' by the immobilized and specifically interacting biomolecules), thus electrochemical determination of antigen binding might be complicated (Wijayawardhana et al., 2000a). Therefore, more practical ways for immunosensor development could be the application of inexpensive glass or plastic substrates for the immobilization of biomolecules and the UME as a sensor for the determination of antigen and antibody interaction, which could be reusable many times. SECM is a technique, which can be used for the determination of antigen and antibody based immune complexes, which are formed at localized surface areas, when one of the interacting biomolecules is immobilized on any kind of surface: transparent, reflecting, conducting or non-conducting. In this case, there is no problem with charge transfer, because antibodies or antigens are immobilized on a surface, which does not act as a signal transducer.

Imaging of immobilized antibody layers with SECM was performed for the first time in 1995 (Wittstock et al., 1995). The oxidised capture anti-digoxin antibody was covalently immobilized on the silanised and activated glass and visualized by SECM after the saturation of the antigen binding sites present in antibody structures with an ALP-antigen conjugate. The enzyme, which was attached to the surface, catalysed a hydrolysis-based conversion of the redox-inactive PAPP into the redox-active PAP, which was determined amperometrically by GC-SECM. However, the most commonly used immunoassay format is the direct sandwich immunoassay, where detecting antibody-HRP conjugates are applied. The common principle of GC-SECM mode used for the detection of an analyte after the interaction with antibody-HRP conjugates is shown in Fig. 5. Here the 'generator' is the enzyme, which is attached to the antibody, and the 'collector' is the UME. A reduced form of the mediator (M_{red}) is added to the solution, and afterwards the redox mediator is oxidised by the enzymes and detected with the UME. Enzymatic reaction takes place only at that areas, where the analyte was bound to the capture antibody and detected using antibody labelled with enzyme.

A direct sandwich immunoassay format was applied for carcinoembryonic antigen (CEA) detection by two SECM modes: FB-SECM and GC-SECM (Shiku et al., 1997). The capture anti-CEA antibodies were microspotted on a silanised glass substrate. CEA present in the solution was attached to the surface *via* affinity interactions with the capture antibody and later detected using an anti-CEA-HRP antibody. The HRP, which was present on the surface, catalysed the oxidation of the redox mediator FcMeOH by H_2O_2. The oxidized form of the redox mediator, which is produced in HRP-catalyzed enzymatic reaction, was detected by the SECM when the UME was located in close proximity to the anti-CEA-HRP-modified surface. The same immunoassay format and conditions were used for a dual immunoassay of human chorionic gonadotropin (HCG) and human placental lactogen (HPL) detection by SECM at a microfabricated glass substrate (Shiku et al., 1997). SECM

was successfully applied for the determination of leucocidin (a toxic protein produced by methicillin-resistant *Staphylococcus aureus*) by an antibody chip, which uses a direct sandwich immunoassay format and detecting anti-leucocidin-HRP antibodies. Capture anti-leucocidin antibodies were site-directed immobilised on protein A-coated glass substrate. The reduction current of the oxidized form of FcMeOH determined by the SECM depended on the concentration of leucocidin bound to anti-leucocidin antibodies (Kasai et al., 2000). A cellular chip based on the direct sandwich immunoassay format combined with a collagen gel embedded cell culture technique for the detection and visualization of cytokines by SECM was developed (Kasai et al., 2006). Simultaneous detection of four tumour markers by protein microarrays was successfully performed using GC-SECM and the redox mediator H_2Q (Fig. 5) (Ning et al., 2018). SECM was applied for a dual and sensitive pepsinogen 1(PEG 1) and pepsinogen 2 (PEG 2) determination using the direct sandwich immunoassay format, detecting antibody labelled with HRP and the redox mediator FcMeOH (Yasukawa et al., 2007).

A direct competitive immunoassay format was used for qualitative and quantitative determination of antibiotic sulfapyridine in milk. In this case antibiotic and its labelled analogue antibiotic-HRP conjugate competed for the antigen binding sites present in capture antibody structure. A site-directed immobilisation of the capture antibody *via* protein G, a competitive immunoassay format and GC-SECM mode involving the reduction of BQ formed during enzymatic reaction ensured a low limit of detection of the antibiotic (Conzuelo et al., 2014). The main advantage of competitive immunoassay is the generation of a higher analytical signal in the presence of lower concentrations of analyte due to the larger quantity of bound antibiotic-HRP conjugates. Some challenging bioanalytical problems, such as sensitivity, specificity, reproducibility, reaction volume and the duration of analysis can be resolved using micro- and nano-particles. Various SECM modes have a potential for the improvement of electrochemical immunoassay characteristics (Ronkainen-Matsuno et al., 2002). Thus, the same (direct competitive) immunoassay format was tested after HRP (antibiotic-HRP conjugate bound to capture antibody) catalysed in-situ deposition of silver nanoparticles (AgNPs). A competition between the UME and the modified carbon plate for the oxidation of ferrocyanide ensured a high contrast in the visualization of deposited AgNPs at the bound antibiotic-HRP sites. A new SECM application strategy for the determination of antigen after enzyme catalysed AgNPs deposition was proved (Conzuelo et al., 2016). Gold nanoparticles as carriers for detecting antibodies and HRP were applied for the enhancement of direct sandwich immunoassay sensitivity for CD10 antigen determination. GC-SECM was used not only for quantitative determination of antigen but also for topographic imaging of antigen and antibody binding event (Song et al., 2012). Magnetic beads were successfully used for the miniaturization of sandwich immunoassay for a mouse-IgG determination by SECM. In this research enzyme ALP that is conjugated to the detecting antibodies, which recognise captured mouse-IgG, catalysed the hydrolysis of PAPP to PAP (redox active product of enzymatic reaction). The activity of ALP over the bead and the anodic current registered by SECM depend on the concentration of the analyte, which is bound to the immobilized antibodies (Wijayawardhana et al., 2000a).

Despite the fact that usually antibodies labelled with enzymes are used for the determination of antigens bound to the capture antibodies and for the imaging by SECM, there are just few publications about the application of SECM in a label-free immunoassay as a potential alternative to fluorescence-based analytical techniques (Holmes et al., 2011). Dotter arrays were fabricated on screen-printed carbon electrodes and biotinylated antibodies were immobilised on neutravidin pre-modified arrays. The binding of antigen was accompanied by an increase of the current registered by SECM using the redox mediator FcCOOH. Such a tendency was explained by an interaction between proteins and redox mediators and increased the localised flux of detectable form of redox mediator. A wide range of different molecular weight antigens (prostate specific antigen (33 kDa), N-terminal cross-linked telopeptide of type I collagen (3 kDa), ciprofloxacin (331 Da)) were tested in SECM-based formats for selective and quantitative binding to dotted immune-arrays (Holmes et al., 2012).

Voltage-switching mode of SECM has been successfully applied for the topographical and electrochemical nanoscale-imaging of living cells (Takahashi et al., 2012). A membrane-bound proteins, such as the epidermal growth factor receptor (EGFR) (one of the key membrane proteins associated with cancer), can be electrochemically determined on a single living cell surface by SECM after the labelling with antibody-ALP conjugate (Takahashi et al., 2009). The same EGFR labelling principle was successfully applied for the investigation of receptor-mediated endocytosis. A marked decrease of current was registered by SECM due to EGF-triggered endocytosis of EGFR (Takahashi et al., 2011).

Usually in immunoassays that are based on antigen and antibody interaction a small volume of biomolecule-containing solution is preferred. Therefore, in such case SECM is a powerful tool, because it can detect proteins immobilized or attached to the surface after specific interaction with proteins immobilised as small spots. A big challenge is to deposit such small drops of solution with biomolecules on the surface. This problem might be solved applying magnetic beads modified by ALP-labelled antibodies. A small 30–100 μm diameter spots formed by attracting these modified particles with a magnet were successfully imaged by SECM in the GC-SECM mode (Wijayawardhana et al. 2000a, 2000b).

4. Conclusions and future trends

SECM is a powerful tool for the investigation of biologically-modified surfaces. Correct selection of an appropriate SECM mode for a particular experiment is a very important issue. Two different SECM modes used for the investigation of the same surface could provide more reliable information. The application of traditional generation-collection mode for the evaluation of enzymes immobilized on the surface or enzyme-labelled antibodies attached to the pre-modified surface *via* affinity interaction is still relatively rare. In this research direction evaluation of new effective redox mediators could provide a break-through in imaging of enzyme-labelled antibodies and the determination of antigens attached to capture antibodies or to membrane-bound receptors after their interaction with antibody-enzyme conjugates. It is expected that in the future SECM will be applied for the evaluation of many biological systems, using new SECM-based approaches and combined techniques.

In the near future the combination of SECM with a fast Fourier transform (FFT) based electrochemical impedance spectroscopy (EIS) seems an extremely powerful combination (FFT-SEIM) of an advanced electrochemical technique, because it can be applied in the presence (Morkvenaite-Vilkonciene et al., 2017a) and in the absence of redox mediators and enables very fast collection of valuable FFT-SEIM.

Declaration of interests

The authors declare that they have no known competing financial interests or personal relationships that could have appeared to influence the work reported in this paper.

CRediT authorship contribution statement

Inga Morkvenaite-Vilkonciene: Conceptualization, Visualization, Writing - original draft, Writing - review & editing. **Almira Ramanaviciene:** Conceptualization, Supervision, Writing - original draft, Writing - review & editing. **Aura Kisieliute:** Writing - original draft, Writing - review & editing. **Vytautas Bucinskas:** Visualization, Writing - original draft, Writing - review & editing. **Arunas Ramanavicius:** Writing - original draft, Writing - review & editing.

Acknowledgements

This research was funded by the European Social Fund (Project No 09.3.3-LMT-K-712-02-0137).

References

Abdul Wahab, R.M., Abu Kasim, N., Senafi, S., Jemain, A.A., Zainol Abidin, I.Z., Shahidan, M.A., Zainal Ariffin, S.H., 2014. Enzyme activity profiles and ELISA analysis of biomarkers from human saliva and gingival crevicular fluid during orthodontic tooth movement using self-ligating brackets. Oral Health Dent. Manag. 13 (2), 194–199.

Alpuche-Aviles, M.A., Wipf, D.O., 2001. Impedance feedback control for scanning electrochemical microscopy. Anal. Chem. 73 (20), 4873–4881.

Arai, T., Nishijo, T., Matsumae, Y., Zhou, Y., Ino, K., Shiku, H., Matsue, T., 2013. Noninvasive measurement of alkaline phosphatase activity in embryoid bodies and coculture spheroids with scanning electrochemical microscopy. Anal. Chem. 85 (20), 9647–9654.

Aranda, P.R., Messina, G.A., Bertolino, F.A., Pereira, S.V., Fernández Baldo, M.A., Raba, J., 2018. Nanomaterials in fluorescent laser-based immunosensors: review and Applications. Microchem. J. 141, 308–323.

Astrauskas, R., Ivanauskas, F., Morkvenaite-Vilkonciene, I., Ramanavicius, A., 2019. Mathematical modelling of the influence of ultra-micro electrode geometry on approach curves registered by scanning electrochemical microscopy. Electroanalysis (accepted for publication).

Ballesteros Katemann, B., Schulte, A., Schuhmann, W., 2003. Constant-distance mode scanning electrochemical microscopy (SECM)–Part I: adaptation of a non-optical shear-force-based positioning mode for SECM tips. Chemistry 9 (9), 2025–2033.

Bard, A.J., Mirkin, M.V., 2001. Scanning Electrochemical Microscopy. Marcel Dekker, NY.

Bard, A.J., Fan, F.R.F., Kwak, J., Lev, O., 1989. Scanning electrochemical microscopy. Introduction and principles. Anal. Chem. 61 (2), 132–138.

Bard, A.J., Mirkin, M.V., Unwin, P.R., Wipf, D.O., 1992. Theory and experiment of the feedback mode with finite heterogeneous electron-transfer kinetics and arbitrary substrate size. J. Phys. Chem. 96 (4), 1861–1868.

Barker, A.L., Gonsalves, M., Macpherson, J.V., Slevin, C.J., Unwin, P.R., 1999. Scanning electrochemical microscopy: beyond the solid/liquid interface. Anal. Chim. Acta 385 (1–3), 223–240.

Brena, B., Gonzalez-Pombo, P., Batista-Viera, F., 2013. Immobilization of enzymes: a literature survey. Methods Mol. Biol. 1051, 15–31.

Burchardt, M., Wittstock, G., 2008. Kinetic studies of glucose oxidase in polyelectrolyte multilayer films by means of scanning electrochemical microscopy (SECM). Bioelectrochemistry 72 (1), 66–76.

Burchardt, M., Träuble, M., Wittstock, G., 2009. Digital simulation of scanning electrochemical microscopy approach curves to enzyme films with Michaelis – Menten kinetics. Anal. Chem. 81 (12), 4857–4863.

Comstock, D.J., Elam, J.W., Pellin, M.J., Hersam, M.C., 2010. Integrated ultramicroelectrode – nanopipet probe for concurrent scanning electrochemical microscopy and scanning ion conductance microscopy. Anal. Chem. 82 (4), 1270–1276.

Conzuelo, F., Stratmann, L., Grützke, S., Pingarrón, J.M., Schuhmann, W., 2014. Detection and quantification of sulfonamide antibiotic residues in milk using scanning electrochemical microscopy. Electroanalysis 26 (3), 481–487.

Conzuelo, F., Grützke, S., Stratmann, L., Pingarrón, J.M., Schuhmann, W., 2016. Interrogation of immunoassay platforms by SERS and SECM after enzyme-catalyzed deposition of silver nanoparticles. Microchim. Acta 183 (1), 281–287.

Cornut, R., Lefrou, C., 2007. A unified new analytical approximation for negative feedback currents with a microdisk SECM tip. J. Electroanal. Chem. 608 (1), 59–66.

Cornut, R., Lefrou, C., 2008. New analytical approximation of feedback approach curves with a microdisk SECM tip and irreversible kinetic reaction at the substrate. J. Electroanal. Chem. 621 (2), 178–184.

Cornut, R., Hapiot, P., Lefrou, C., 2009. Enzyme-mediator kinetics studies with SECM: numerical results and procedures to determine kinetics constants. J. Electroanal. Chem. 633 (1), 221–227.

Csoka, B., Kovacs, B., Nagy, G., 2003. Investigation of concentration profiles inside operating biocatalytic sensors with scanning electrochemical microscopy (SECM). Biosens. Bioelectron. 18 (2–3), 141–149.

Eckhard, K., Chen, X., Turcu, F., Schuhmann, W., 2006. Redox competition mode of scanning electrochemical microscopy (RC-SECM) for visualisation of local catalytic activity. Phys. Chem. Chem. Phys. 8 (45), 5359–5365.

Eckhard, K., Shin, H., Mizaikoff, B., Schuhmann, W., Kranz, C., 2007. Alternating current (AC) impedance imaging with combined atomic force scanning electrochemical microscopy (AFM-SECM). Electrochem. Commun. 9 (6), 1311–1315.

Edelson, J.D., Shannon, J.M., Mason, R.J., 1988. Alkaline phosphatase: a marker of alveolar type II cell differentiation. Am. Rev. Respir. Dis. 138 (5), 1268–1275.

Evans, S.A.G., Brakha, K., Billon, M., Mailley, P., Denuault, G., 2005. Scanning electrochemical microscopy (SECM): localized glucose oxidase immobilization via the direct electrochemical microspotting of polypyrrole-biotin films. Electrochem. Commun. 7 (2), 135–140.

Fan, H., Jiao, F., Chen, H., Zhang, F., Wang, Q., He, P., Fang, Y., 2013. Qualitative and quantitative detection of DNA amplified with HRP-modified SiO_2 nanoparticles using scanning electrochemical microscopy. Biosens. Bioelectron. 47 (0), 373–378.

Gdor, E., Katz, E., Mandler, D., 2013. Biomolecular and logic gate based on immobilized enzymes with precise spatial separation controlled by scanning electrochemical microscopy. J. Phys. Chem. B 117 (50), 16058–16065.

Glidle, A., Yasukawa, T., Hadyoon, C.S., Anicet, N., Matsue, T., Nomura, M., Cooper, J.M., 2003. Analysis of protein adsorption and binding at biosensor polymer interfaces using X-ray photon spectroscopy and scanning electrochemical microscopy. Anal. Chem. 75 (11), 2559–2570.

Guadagnini, L., Maljusch, A., Chen, X., Neugebauer, S., Tonelli, D., Schuhmann, W., 2009. Visualization of electrocatalytic activity of microstructured metal hexacyanoferrates by means of redox competition mode of scanning electrochemical microscopy (RC-SECM). Electrochim. Acta 54 (14), 3753–3758.

Gyurcsányi, R.E., Jágerszki, G., Kiss, G., Tóth, K., 2004. Chemical imaging of biological systems with the scanning electrochemical microscope. Bioelectrochemistry 63 (1–2), 207–215.

Hengstenberg, A., Kranz, C., Schuhmann, W., 2000. Facilitated tip-positioning and applications of non-electrode tips in scanning electrochemical microscopy using a shear force based constant-distance mode. Chem. Eur J. 6 (9), 1547–1554.

Holmes, J.L., Davis, F., Collyer, S.D., Higson, S.P., 2011. A new application of scanning electrochemical microscopy for the label-free interrogation of antibody–antigen interactions: Part 1. Anal. Chim. Acta 689 (2), 206–211.

Holmes, J.L., Davis, F., Collyer, S.D., Higson, S.P.J., 2012. A new application of scanning electrochemical microscopy for the label-free interrogation of antibody–antigen interactions: Part 2. Anal. Chim. Acta 741, 1–8.

Horrocks, B.R., Schmidtke, D., Heller, A., Bard, A.J., 1993. Scanning electrochemical microscopy. 24. Enzyme ultramicroelectrodes for the measurement of hydrogen peroxide at surfaces. Anal. Chem. 65 (24), 3605–3614.

Huang, L., Li, Z., Lou, Y., Cao, F., Zhang, D., Li, X., Huang, L., Li, Z., Lou, Y., Cao, F., Zhang, D., Li, X., 2018. Recent advances in scanning electrochemical microscopy for biological applications. Materials 11 (8), 1389.

Ivanauskas, F., Morkvenaite-Vilkonciene, I., Astrauskas, R., Ramanavicius, A., 2016. Modelling of scanning electrochemical microscopy at redox competition mode using diffusion and reaction equations. Electrochim. Acta 222, 347–354.

Izquierdo, J., Knittel, P., Kranz, C., 2018. Scanning electrochemical microscopy: an analytical perspective. Anal. Bioanal. Chem. 410 (2), 307–324.

James, P.I., Garfias-Mesias, L.F., Moyer, P.J., Smyrl, W.H., 1998. Scanning electrochemical microscopy with simultaneous independent topography. J. Electrochem. Soc. 145 (4), L64–L66.

Kai, T., Zoski, C.G., Bard, A.J., 2018. Scanning electrochemical microscopy at the nanometer level. Chem. Commun. 54 (16), 1934–1947.

Kasai, S., Yokota, A., Zhou, H., Nishizawa, M., Niwa, K., Onouchi, T., Matsue, T., 2000. Immunoassay of the MRSA-related toxic protein, leukocidin, with scanning electrochemical microscopy. Anal. Chem. 72 (23), 5761–5765.

Kasai, S., Hirano, Y., Motochi, N., Shiku, H., Nishizawa, M., Matsue, T., 2002. Simultaneous detection of uric acid and glucose on a dual-enzyme chip using scanning electrochemical microscopy/scanning chemiluminescence microscopy. Anal. Chim. Acta 458 (2), 263–270.

Kasai, S., Shiku, H., Torisawa, Y.-s., Nagamine, K., Yasukawa, T., Watanabe, T., Matsue, T., 2006. Cytokine assay on a cellular chip by combining collagen gel embedded culture with scanning electrochemical microscopy. Anal. Chim. Acta 566 (1), 55–59.

Khan, G.F., Wernet, W., 1997. Design of enzyme electrodes for extended use and storage life. Anal. Chem. 69 (14), 2682–2687.

Kranz, C., Kueng, A., Lugstein, A., Bertagnolli, E., Mizaikoff, B., 2004. Mapping of enzyme activity by detection of enzymatic products during AFM imaging with integrated SECM–AFM probes. Ultramicroscopy 100 (3–4), 127–134.

Kuo, T.-R., Chen, C.-H., 2017. Bone biomarker for the clinical assessment of osteoporosis: recent developments and future perspectives. Biomark. Res. 5 18-18.

Laschi, S., Palchetti, I., Marrazza, G., Mascini, M., 2009. Enzyme-amplified electrochemical hybridization assay based on PNA, LNA and DNA probe-modified micromagnetic beads. Bioelectrochemistry 76 (1), 214–220.

Lei, R., Stratmann, L., Schafer, D., Erichsen, T., Neugebauer, S., Li, N., Schuhmann, W., 2009. Imaging biocatalytic activity of enzyme-polymer spots by means of combined scanning electrochemical microscopy/electrogenerated chemiluminescence. Anal. Chem. 81 (12), 5070–5074.

Li, J.P., Yu, J.G., 2008. Fabrication of Prussian Blue modified ultramicroelectrode for GOD imaging using scanning electrochemical microscopy. Bioelectrochemistry 72 (1), 102–106.

Li, W., Yuan, R., Chai, Y., Zhou, L., Chen, S., Li, N., 2008. Immobilization of horseradish peroxidase on chitosan/silica sol–gel hybrid membranes for the preparation of hydrogen peroxide biosensor. J. Biochem. Biophys. Methods 70 (6), 830–837.

Lin, T.E., Rapino, S., Girault, H.H., Lesch, A., 2018. Electrochemical imaging of cells and tissues. Chem. Sci. 9 (20), 4546–4554.

Loaiza, O.A., Campuzano, S., de Prada, A.G.-V., Pedrero, M., Pingarrón, J.M., 2008. Amperometric DNA quantification based on the use of peroxidase-mercaptopropionic acid-modified gold electrodes. Sensor. Actuator. B 132 (1), 250–257.

Lou, D., Fan, L., Cui, Y., Zhu, Y., Gu, N., Zhang, Y., 2018. Fluorescent nanoprobes with oriented modified antibodies to improve lateral flow immunoassay of cardiac Troponin I. Anal. Chem. 90 (11), 6502–6508.

Ludwig, M., Kranz, C., Schuhmann, W., Gaub, H.E., 1995. Topography feedback mechanism for the scanning electrochemical microscope based on hydrodynamic forces between tip and sample. Rev. Sci. Instrum. 66 (4), 2857–2860.

Macpherson, J.V., Unwin, P.R., Hillier, A.C., Bard, A.J., 1996. In-situ smaging of sonic crystal dissolution using an integrated electrochemical/AFM probe. J. Am. Chem. Soc. 118 (27), 6445–6452.

Mohamad, N.R., Marzuki, N.H.C., Buang, N.A., Huyop, F., Wahab, R.A., 2015. An overview of technologies for immobilization of enzymes and surface analysis techniques for immobilized enzymes. Biotechnol. Biotechnol. Equip. 29 (2), 205–220.

Morkvenaite-Vilkonciene, I., Ramanaviciene, A., Ramanavicius, A., 2014. Redox competition and generation-collection modes based scanning electrochemical microscopy for the evaluation of immobilised glucose oxidase-catalysed reactions. RSC Adv. 4 (91), 50064–50069.

Morkvenaite-Vilkonciene, I., Genys, P., Ramanaviciene, A., Ramanavicius, A., 2015. Scanning electrochemical impedance microscopy for investigation of glucose oxidase catalyzed reaction. Colloids Surf., B 126, 598–602.
Morkvenaite-Vilkonciene, I., Valiūnienė, A., Petroniene, J., Ramanavicius, A., 2017a. Hybrid system based on fast Fourier transform electrochemical impedance spectroscopy combined with scanning electrochemical microscopy. Electrochem. Commun. 83, 110–112.
Morkvenaite Vilkonciene, I., Ramanaviciene, A., Genys, P., Ramanavicius, A., 2017b. Evaluation of enzymatic kinetics of GOx-based electrodes by scanning electrochemical microscopy at redox competition mode. Electroanalysis 29 (6), 1532–1542.
Nebel, M., Eckhard, K., Erichsen, T., Schulte, A., Schuhmann, W., 2010. 4D Shear force-based constant-distance mode scanning electrochemical microscopy. Anal. Chem. 82 (18), 7842–7848.
Nebel, M., Grutzke, S., Diab, N., Schulte, A., Schuhmann, W., 2013a. Microelectrochemical visualization of oxygen consumption of single living cells. Faraday Discuss 164, 19–32.
Nebel, M., Grützke, S., Diab, N., Schulte, A., Schuhmann, W., 2013b. Visualization of oxygen consumption of single living cells by scanning electrochemical microscopy: the influence of the Faradaic tip reaction. Angew. Chem. Int. Ed. 52 (24), 6335–6338.
Ning, X., Xiong, Q., Zhang, F., He, P., 2018. Simultaneous detection of tumor markers in lung cancer using scanning electrochemical microscopy. J. Electroanal. Chem. 812, 101–106.
Nogala, W., Szot, K., Burchardt, M., Roelfs, F., Rogalski, J., Opallo, M., Wittstock, G., 2010. Feedback mode SECM study of laccase and bilirubin oxidase immobilised in a sol–gel processed silicate film. Analyst 135 (8), 2051.
Pellissier, M., Zigah, D., Barriere, F., Hapiot, P., 2008. Optimized preparation and scanning electrochemical microscopy analysis in feedback mode of glucose oxidase layers grafted onto conducting carbon surfaces. Langmuir 24 (16), 9089–9095.
Pierce, D.T., Unwin, P.R., Bard, A.J., 1992. Scanning electrochemical microscopy. 17. Studies of enzyme-mediator kinetics for membrane- and surface-immobilized glucose oxidase. Anal. Chem. 64 (17), 1795–1804.
Ramanaviciene, A., German, N., Kausaite-Minkstimiene, A., Voronovic, J., Kirlyte, J., Ramanavicius, A., 2012. Comparative study of surface plasmon resonance, electrochemical and electroassisted chemiluminescence methods based immunosensor for the determination of antibodies against human growth hormone. Biosens. Bioelectron. 36 (1), 48–55.
Roberts, W.S., Lonsdale, D.J., Griffiths, J., Higson, S.P., 2007. Advances in the application of scanning electrochemical microscopy to bioanalytical systems. Biosens. Bioelectron. 23 (3), 301–318.
Roberts, W.S., Davis, F., Collyer, S.D., Higson, S.P., 2011. Construction and interrogation of enzyme microarrays using scanning electrochemical microscopy–optimisation of adsorption and determination of enzymatic activity. Analyst 136 (24), 5287–5293.
Ronkainen-Matsuno, N.J., Thomas, J.H., Halsall, H.B., Heineman, W.R., 2002. Electrochemical immunoassay moving into the fast lane. Trends Anal. Chem. 21 (4), 213–225.
Schafer, D., Puschhof, A., Schuhmann, W., 2013. Scanning electrochemical microscopy at variable temperatures. Phys. Chem. Chem. Phys. 15 (14), 5215–5223.
Shiku, H., Matsue, T., Uchida, I., 1996. Detection of microspotted carcinoembryonic antigen on a glass substrate by scanning electrochemical microscopy. Anal. Chem. 68 (7), 1276–1278.
Shiku, H., Hara, Y., Matsue, T., Uchida, I., Yamauchi, T., 1997. Dual immunoassay of human chorionic gonadotropin and human placental lactogen at a miocrofabricated substrate by scanning electrochemical microscopy. J. Electroanal. Chem. 438 (1–2), 187–190.
Shiku, H., Shiraishi, T., Ohya, H., Matsue, T., Abe, H., Hoshi, H., Kobayashi, M., 2001. Oxygen consumption of single bovine embryos probed by scanning electrochemical microscopy. Anal. Chem. 73 (15), 3751–3758.
Shin, H., Hesketh, P.J., Mizaikofff, B., Kranz, C., 2008. Development of wafer-level batch fabrication for combined atomic force-scanning electrochemical microscopy (AFM-SECM) probes. Sensor. Actuator. B Chem. 134 (2), 488–495.
Song, W., Yan, Z., Hu, K., 2012. Electrochemical immunoassay for CD10 antigen using scanning electrochemical microscopy. Biosens. Bioelectron. 38 (1), 425–429.
Sun, T., Wang, D., Mirkin, M.V., 2018. Tunneling mode of scanning electrochemical microscopy: probing electrochemical processes at single nanoparticles. Angew. Chem. Int. Ed. 57 (25), 7463–7467.
Szunerits, S., Knorr, N., Calemczuk, R., Livache, T., 2004. New approach to writing and simultaneous reading of micropatterns: combining surface plasmon resonance imaging with scanning electrochemical microscopy (SECM). Langmuir 20 (21), 9236–9241.
Takahashi, Y., Shevchuk, A.I., Novak, P., Babakinejad, B., Macpherson, J., Unwin, P.R., Shiku, H., Gorelik, J., Klenerman, D., Korchev, Y.E., Matsue, T., 2012. Topographical and electrochemical nanoscale imaging of living cells using voltage-switching mode scanning electrochemical microscopy. Proc. Natl. Acad. Sci. U. S. A 109, 11540–11545.
Takahashi, Y., Miyamoto, T., Shiku, H., Asano, R., Yasukawa, T., Kumagai, I., Matsue, T., 2009. Electrochemical detection of epidermal growth factor receptors on a single living cell surface by scanning electrochemical microscopy. Anal. Chem. 81, 2785–2790.
Tang, H.T., Lunte, C.E., Halsall, H.B., Heineman, W.R., 1988. p-aminophenyl phosphate: an improved substrate for electrochemical enzyme immnoassay. Anal. Chim. Acta 214, 187–195.
Teranishi, R., Higuchi, E., Chiku, M., Inoue, H., 2011. Analysis of kinetics of oxygen reduction reaction in alkaline solution by scanning electrochemical microscopy. Bioelectrocatalysis 41 (1), 2179–2184.
Torisawa, Y.-S., Ohara, N., Nagamine, K., Kasai, S., Yasukawa, T., Shiku, H., Matsue, T., 2006. Electrochemical monitoring of cellular signal transduction with a secreted alkaline phosphatase reporter system. Anal. Chem. 78 (22), 7625–7631.
Treutler, T.H., Wittstock, G., 2003. Combination of an electrochemical tunneling microscope (ECSTM) and a scanning electrochemical microscope (SECM): application for tip-induced modification of self-assembled monolayers. Electrochim. Acta 48 (20–22), 2923–2932.
Wijayawardhana, C.A., Wittstock, G., Halsall, H.B., Heineman, W.R., 2000a. Electrochemical immunoassay with microscopic immunomagnetic bead domains and scanning electrochemical microscopy. Electroanalysis 12 (9), 640–644.
Wijayawardhana, C.A., Wittstock, G., Halsall, H.B., Heineman, W.R., 2000b. Spatially addressed deposition and imaging of biochemically active bead microstructures by scanning electrochemical microscopy. Anal. Chem. 72 (2), 333–338.
Wilhelm, T., Wittstock, G., 2003. Analysis of interaction in patterned multienzyme layers by using scanning electrochemical microscopy. Angew. Chem. Int. Ed. 42 (20), 2248–2250.
Wittstock, G., 2001. Modification and characterization of artificially patterned enzymatically active surfaces by scanning electrochemical microscopy. Fresenius J. Anal. Chem. 370 (4), 303–315.
Wittstock, G., Schuhmann, W., 1997. Formation and imaging of microscopic enzymatically active spots on an alkanethiolate-covered gold electrode by scanning electrochemical microscopy. Anal. Chem. 69 (24), 5059–5066.
Wittstock, G., Yu, K.J., Halsall, H.B., Ridgway, T.H., Heineman, W.R., 1995. Imaging of immobilized antibody layers with scanning electrochemical microscopy. Anal. Chem. 67 (19), 3578–3582.
Wittstock, G., Burchardt, M., Pust, S.E., Shen, Y., Zhao, C., 2007. Scanning electrochemical microscopy for direct imaging of reaction rates. Angew. Chem. Int. Ed. 46, 1584–1617.
Yang, Y., Yan, Q., Liu, Q., Li, Y., Liu, H., Wang, P., Chen, L., Zhang, D., Li, Y., Dong, Y., 2018. An ultrasensitive sandwich-type electrochemical immunosensor based on the signal amplification strategy of echinoidea-shaped Au@Ag-Cu_2O nanoparticles for prostate specific antigen detection. Biosens. Bioelectron. 99, 450–457.
Yasukawa, T., Hirano, Y., Motochi, N., Shiku, H., Matsue, T., 2007. Enzyme immunosensing of pepsinogens 1 and 2 by scanning electrochemical microscopy. Biosens. Bioelectron. 22 (12), 3099–3104.
Zhang, Z., Zhou, J., Tang, A., Wu, Z., Shen, G., Yu, R., 2010. Scanning electrochemical microscopy assay of DNA based on hairpin probe and enzymatic amplification biosensor. Biosens. Bioelectron. 25 (8), 1953–1957.
Zhao, C., Wittstock, G., 2005. Scanning electrochemical microscopy for detection of biosensor and biochip surfaces with immobilized pyrroloquinoline quinone (PQQ)-dependent glucose dehydrogenase as enzyme label. Biosens. Bioelectron. 20 (7), 1277–1284.
Zhou, J.F., Campbell, C., Heller, A., Bard, A.J., 2002. Scanning electrochemical microscopy. 44. Imaging of horseradish peroxidase immobilized on insulating substrates. Anal. Chem. 74 (16), 4007–4010.